JOURNAL OF FORENSIC SCIENCES

J Forensic Sci, January 2014, Vol. 59, No. 1
doi: 10.1111/1556-4029.12294
Available online at: onlinelibrary.wiley.com

PAPER

CRIMINALISTICS

Dana Bors,[1] *B.S.; Josh Cummins,*[1] *B.S.; and John Goodpaster,*[1] *Ph.D.*

The Anatomy of a Pipe Bomb Explosion: Measuring the Mass and Velocity Distributions of Container Fragments

ABSTRACT: Improvised explosive devices such as pipe bombs are prevalent due to the availability of materials and ease of construction. However, little is known about how these devices actually explode, as few attempts to characterize fragmentation patterns have been attempted. In this study, seven devices composed of various pipe materials (PVC, black steel, and galvanized steel) and two energetic fillers (Pyrodex and Alliant Red Dot) were initiated and the explosions captured using high-speed videography. The video footage was used to calculate fragment velocities, which were represented as particle velocity vector maps. In addition, the fragments were weighed. The results demonstrate a correlation between the type of energetic filler and both the size and velocity of the fragments. Larger fragments were produced by Pyrodex filler indicating a less complete fragmentation, compared with smaller fragments produced by double-base smokeless powder. Additionally, higher fragment velocities were seen with Alliant Red Dot filler.

KEYWORDS: forensic science, explosives, pipe bomb, fragmentation, smokeless powder, high-speed video

Pipe bombs are a common type of improvised explosive device (IED) that can be constructed of readily available materials found at local hardware and sporting goods stores. Pipe bombs typically contain deflagrating low explosive powders (i.e., black powder, black powder substitutes, and smokeless powder). As pipe bombs utilize low explosives as the main charge, the pipe serves as a rigid container that confines the deflagration until the pipe expands and eventually fails, resulting in an explosion. Although pipe bombs are crude in design, they can also be quite lethal. For example, during a demonstration of civil unrest in Northern Ireland, a pipe bomb killed a 16-year-old boy as he raised his arm to throw it. His hand was severely mangled and nearly amputated. Shrapnel gashed the back of his head exposing fractured skull and brain matter (1). Ted Kaczynski, commonly known as the Unabomber, killed Hugh Scrutton using a pipe bomb packed with nails (2). Furthermore, pipe bombs constitute the bulk of the United States' bombing incidents. Since 1978, the US Bureau of Alcohol, Tobacco, Firearms, and Explosives (ATF) has reported 32,000 bombings and attempted bombings, as well as 23,500 incidents with recovered explosives or devices (3).

The pipes used in pipe bombs are typically made of polyvinyl chloride (PVC), chlorinated polyvinyl chloride (CPVC), black steel, or galvanized steel. Given that such pipes are intended for use in plumbing applications, they conform to a number of standards and conventions. For example, the outer diameters of all commercially available pipes must conform to a nominal pipe size that does not always match the actual outer diameter (e.g., a one-inch nominal diameter pipe is actually 1.315 inches in outer diameter). In addition, the wall thickness of pipe is dictated by schedules, with one of the most common being Schedule 40 (e.g., a one-inch nominal diameter Schedule 40 pipe must have walls that are 0.133 inches thick).

The protocols for the laboratory examination of a pipe bomb that has either been rendered safe or functioned as designed will vary depending upon the laboratory involved. However, one can generalize these protocols into three main stages: an initial visual/microscopic examination to photograph and document the evidence, chemical analysis to identify any intact explosive particles or residues that may be present, and an examination of any device components that may be present.

Much time and attention has been focused on the second stage of this process. For example, chemical and instrumental methods for identifying low explosives and their postblast residues are well established and described in various books and book chapters (4–7). The third stage, the identification and comparison of IED components, is also well established as it involves many of the same analytical techniques applied to items such as tape, fuses, wires, batteries, etc. In contrast, only a small amount of published research is available that is focused on the first stage of this process. This stage, although necessarily presumptive in nature, is no less important given that the types of analyses required for different explosive fillers can vary dramatically. A well-formed hypothesis can help direct subsequent examinations and adds probative value by linking direct observations with instrumental results.

In particular, during a visual/microscopic examination, one can begin to formulate a hypothesis as to the explosive filler based upon the size, shape, and number of container fragments that are present. For example, steel pipe bombs containing black

[1]Forensic and Investigative Sciences Program, Department of Chemistry and Chemical Biology, Indiana University Purdue University Indianapolis (IUPUI), 402 North Blackford Street, Indianapolis, IN 46202.

Received 3 Aug. 2012; and in revised form 15 Nov. 2012; accepted 14 Dec. 2012.

powder or black powder substitutes will produce few large fragments. The end cap face plates are often blown out, and fragments will exhibit square, 90° edges. Heavy gray or black residue will be present on the interior surfaces of the pipe. Finally, the pipe may be rusted due to the formation of corrosive by-products. In contrast, steel pipe bombs containing double-base smokeless powder (DBSP) will have no apparent residue. There will be extensive fragmentation, including 90° breaks as well as 45° reversing slants on edges (this is known as "stepping"). Finally, the pipe fragments may be thinned due to the force of the explosion.

These characteristics are based upon the extensive experience of forensic chemists, but they also draw support from many decades of research into the behavior of cylindrical explosive devices. Although many of these studies were focused on military high explosives, their general conclusions are still useful and many of their observations are also seen in pipe bombs filled with highly energetic low explosives such as DBSP. For example, Taylor and others investigated the effect of tensile and compressive stress on fracture radii, concluding a proportional relationship (8,9). Tensile stress is the tension that results when materials resist elongation as equal and opposite forces are applied to them. Compressive stress is tension in multiple directions acting on a material causing shortening. These stresses both influence the extent to which a tube can expand before it begins to fracture. With the inclusion of detonation pressure as a variable, it was found that the diameter of a tube expands to nearly twice the original size before fragmentation occurs. This, in turn, leads to thinning of the container walls. The first fractures appear along planes of maximum shear stress, usually along the longitudinal axis (10). Stepping, also called a shear lip fracture, is also present when high pressures are generated inside the device (10).

Computational modeling of cylinders by Anderson explains that the majority of the velocity of casing fragments is obtained before fragmentation occurs (11). In other words, the acceleration of the tube material is most active when the tube is still intact. Furthermore, following fragmentation of a cylindrical device, a correlation exists between a fragment's projection angle and its speed, as well as the detonation velocity of the bomb:

$$\theta = \sin^{-1}\left(\frac{V_0}{2U}\right) \tag{1}$$

where θ is the angle relative to the normal to the surface, V_0 is the speed, and U is the detonation velocity (12). This formula is valid when flow is largely one dimensional, common with long artillery projectiles. Finally, Gurney developed an equation that relates initial fragment velocity to properties of the explosive and container:

$$V_0 = (2E')^{1/2} \times \left(\frac{W/W_c}{1 + (W/2W_c)}\right)^{1/2} \tag{2}$$

where V_0 is the initial fragment velocity, $(2E')^{1/2}$ is the Gurney constant, W is the weight of the explosive, and W_c is the weight of the casing (4). The Gurney energy constant varies with explosive type and is usually about one-third of the value of the detonation velocity (13). This equation is also only effective for one-dimensional flow, and some circumstances require more detailed calculations.

Overall, this summary shows that while the investigation of fragmentation patterns and velocities is not new, there is a need to apply these and other methods to low explosive devices used by amateurs. On the other hand, attempts to characterize IEDs using the mass of postblast fragments with respect to container type and filler energy have been demonstrated, most notably by Oxley (14). Fragment Weight Distribution Maps (FWDMs), used by Oxley, were employed to characterize the distribution of fragment masses. Constructing a FWDM involves plotting the relative mass of a given fragment versus the mass of that fragment divided by the mass of all fragments of higher mass (14).

Equation 3 is the equation for plotting the FWDMs where M_r = the mass of the n*th* fragment plus all fragments heavier than the n*th* fragment, M_n = the mass of the n*th* fragment, M_{total} = the total mass of all fragments collected, and m = slope. In practice, a value of two is added to the y-axis component of the equation to assure that FWDMs reside in the first quadrant graphically.

$$\log\left(M_r/M_{\text{total}}\right) = m\left(M_n/M_{\text{total}}\right) \tag{3}$$

It is important to note that Oxley's experiments utilized secondary containers to recover as much of the pipe fragments as possible. However, an FWDM is intended to be relatively insensitive to fragment recovery percentage, making this an attractive characterization method.

The use of FWDMs as a forensic tool has been challenged by Dean (15), who claims that the proportion of fragments recovered should not be used as a quantitative measure. In other words, as both the ordinate and abscissa of the FWDM are normalized by the total number of fragments recovered, the slope is still considered to be slightly dependent on the total recovery. Because of this, bias will be present based on the total fragments recovered; therefore, using a proportion of fragments for characterization purposes is inaccurate. Following this reasoning, the Held equation, specifically the constant B, is rejected as a valid quantitative method as well. The constant B is a function of the total mass recovered in addition to the mass of the largest fragment, yielding misleading data if the total recovery is reduced (15). The Held equation is:

$$M(n) = M_0 * \left[1 - e^{-Bn^{\lambda}}\right] \tag{4}$$

where $M(n)$ is the cumulative fragment mass or the overall mass of the heaviest n fragments, M_0 is the total mass of all fragments, n is the cumulative fragment number beginning with the heaviest fragment, and B and λ are constants(16).

Besides mass, other physical characteristics of container fragments have been examined. This has included microstructure deformation and hardness, to correlate explosive properties with material response. Walsh concludes that as the detonation pressure and velocity increase, microstructure deformation increases as well, to the point of localized recrystallization in some cases (17). At low detonation velocities and pressure, the hardness increased immediately, compared with a plateau at medium velocities and a decrease in hardness with high energy fillers. Gregory expanded on Walsh's qualitative study, in an attempt to produce quantitative results. Work hardening was monitored by microhardness, specifically in the form of Knoop hardness values. Values increased with increasing energy fillers, also causing a large aspect ratio due to pearlite deformation (18). Pipe thinning was directly correlated with the amount of plastic deformation

caused by the resulting pressure wave; therefore, the use of a high energy filler would result in a decrease of pipe thickness.

Overall, it is our opinion that the potential for pipe bomb fragments to injure or kill is not fully appreciated. In addition, the lethality of pipe bombs that do not contain shrapnel is largely based upon the velocity and mass of container fragments leaving the site of a pipe bomb explosion. Hence, we have measured the velocity and mass of pipe bomb container fragments using a high-speed video camera and an analytical balance, respectively. The aim of this study is to demonstrate the major trends that exist for various container types (e.g., PVC, black steel and galvanized steel) as well as filler (e.g., Pyrodex and DBSP). In particular, our hypothesis is that fragment mass distributions (expressed as either simple histograms or FWDM slopes) can indicate the explosive filler and that the velocity of fragments will be proportional to the explosive power of the filler. We will also display velocity data in the form of particle velocity vector maps (PVVMs), which are displayed as the paths or tracks taken by the fragments overlaid on top of a representation of the pipe bomb. In addition, our results include a surprising anomaly in the slopes of our FWDM plots as well as a larger than expected distribution of fragment velocities.

Materials and Methods

A total of seven devices were exploded. For all devices, the explosive filler was either Hodgdon Pyrodex or Alliant Red Dot DBSP. All devices were constructed from eight-inch lengths of one-inch nominal diameter Schedule 40 pipe. These pipes were constructed from galvanized steel, black steel (steel pipe with a black lacquer coating), and PVC, respectively. All devices were capped at both ends with the corresponding material type. For the metal devices, endcaps were composed of cast iron, rather than milled steel. One end cap was drilled on each device with a 3/16 inch hole to accommodate the igniter wires.

All devices were assembled and initiated via electric match (seen on the right in all videos). The Indiana State Police Bomb Squad assembled and exploded the devices in a gravel pit in Noblesville, IN. Two containment structures, one for each filler type, were constructed with dimensions of approximately 8 ft. × 8 ft. × 4 ft. from 3/4-inch plywood. Each device was suspended from a lumber strut via fishing line, so that the IED was approximately two feet from the ground (Fig. 1).

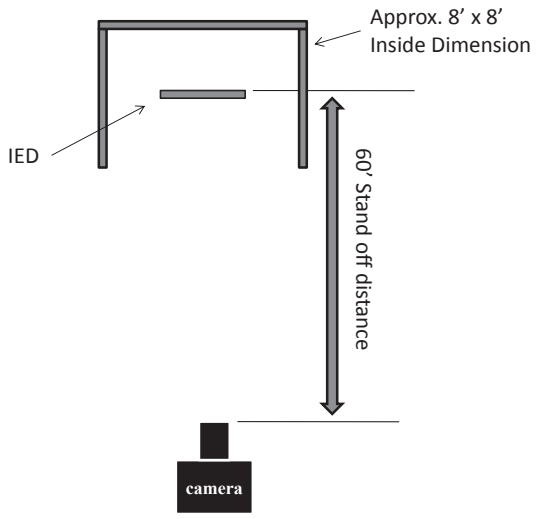

FIG. 1—*Schematic of the experimental setup.*

The first two devices consisted of a PVC pipe filled with DBSP. These were used to validate the frame rate (10,000 frames per second) and shutter speed (19.6 μs) of the high-speed video camera. These parameters were then used on each of the successive devices. The videos that captured the explosions were analyzed using ProAnalyst software (Xcitex, Cambridge, MA). Individual fragments were tracked within the software, and their velocity was calculated by plotting the XY position (in pixels) of the fragment as a function of time to yield a velocity in pixels per second. The velocities were then converted from pixels per seconds to inches per seconds by calculating the number of pixels per inch for the outer diameter of the pipe (1.315 inches), which was visible in the footage prior to the blast. The velocities of individual fragments were then plotted using PVVMs. Particle velocity vector maps depict a two-dimensional representation of the IED, along with numerous fragments whose trajectories could be tracked in the high-speed video footage.

It is important to note that due to the geometry of the camera setup, all fragments were tracked only in two dimensions. Given that fragments can travel in and out of the plane of focus for the camera, all velocity values are *minimum* estimates. The following equation depicts the relationship between velocities obtained from the high-speed imaging and the actual velocities:

$$\text{Actual} = \text{measured}/\cos\theta \tag{5}$$

In future work, it is hoped to utilize two cameras to simultaneously record the event and then reconstruct a three-dimensional trajectory for container fragments, thereby avoiding this source of error.

Postblast fragments were collected and placed into cans corresponding to pipe material type and filler. All personnel wore latex gloves to prevent cross-contamination. Postblast fragment masses were recorded using a Fisher Scientific analytical balance (Accuseries-124; Pittsburgh, PA). The distribution of fragment masses was visualized using histograms and FWDMs with respect to container and filler type.

Results and Discussion

Visual and Microscopic Examination

The fragment edge profiles were analyzed via visual inspection and photography either by digital camera or stereomicroscope when greater magnification was needed. The PVC IEDs regardless of filler generated many small fragments, and all containers were completely destroyed. However, there was a difference between the size of fragments between the low-power and high-power fillers with smaller fragments for the Alliant Red Dot Devices than for the Pyrodex devices.

The metallic devices filled with Pyrodex produced fragments that were relatively large, thus leaving fewer to collect. Many of these devices only generated end cap fragments and very small number of body fragments typically leaving a large portion of the device intact. The edge profiles of these fragments for the most part demonstrated a 90° break with respect to the exterior surface of the device.

In contrast, the higher energy filler, Alliant Red Dot, generated much smaller fragments and destroyed most of the device upon explosion. The fragment edge profiles for these devices were jagged and demonstrated a classic saw-tooth-like pattern typically seen in high explosive container fragments known as *stepping*. Transitions between smooth 90° edges and stepped

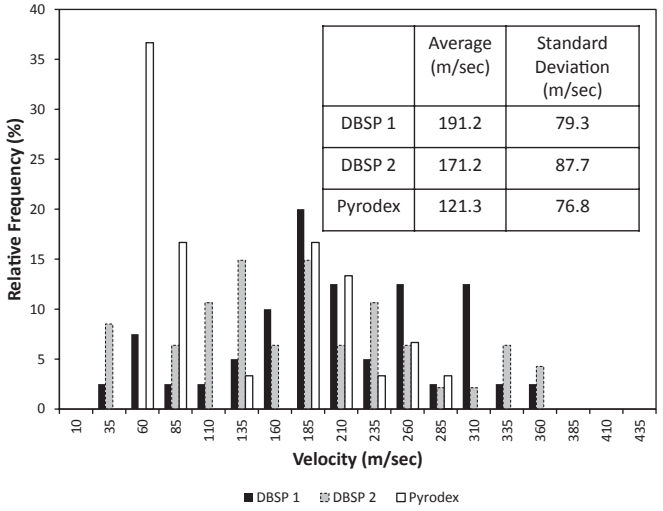

	Average (m/sec)	Standard Deviation (m/sec)
DBSP 1	191.2	79.3
DBSP 2	171.2	87.7
Pyrodex	121.3	76.8

FIG. 2—*Histogram of fragment velocities from PVC devices filled with either double-base smokeless powder (DBSP) or Pyrodex.*

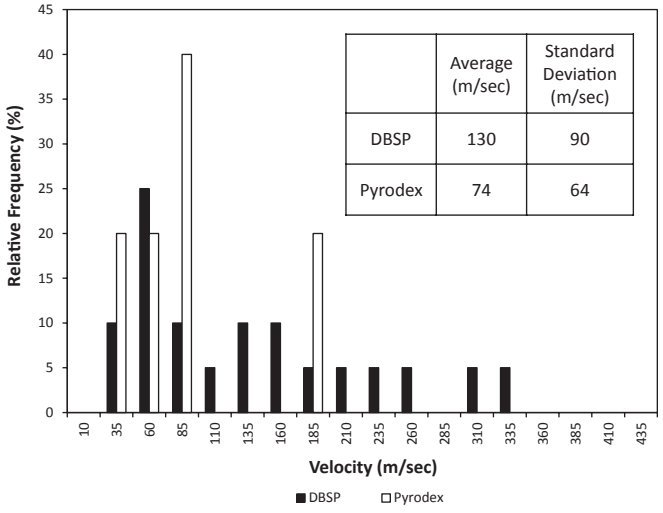

	Average (m/sec)	Standard Deviation (m/sec)
DBSP	130	90
Pyrodex	74	64

FIG. 3—*Histogram of fragment velocities from black steel devices filled with either double-base smokeless powder (DBSP) or Pyrodex.*

edges on some of the larger fragments can be seen in some of these metallic fragments.

Velocity Measurements

Histograms were used to graphically display the distribution of fragment velocities from devices constructed from PVC, black steel, and galvanized steel (Figs 2–4). For example, Fig. 2 shows the distribution of velocities for the three PVC devices. The two PVC devices with DBSP filler exhibited a near Gaussian distribution of velocities with similar means. In contrast, the PVC device with Pyrodex filler had more fragments traveling at lower velocities as well as a wider range of overall velocities. Figures 3 and 4 show the distribution of velocities for the black steel and galvanized steel devices, respectively. In both cases, Pyrodex filler generated fragments with lower velocities, whereas the devices with DBSP filler generated fragments with higher average velocities that spanned a very wide range. In comparison, the Pyrodex filler generated lower velocities that were more clustered around a central point.

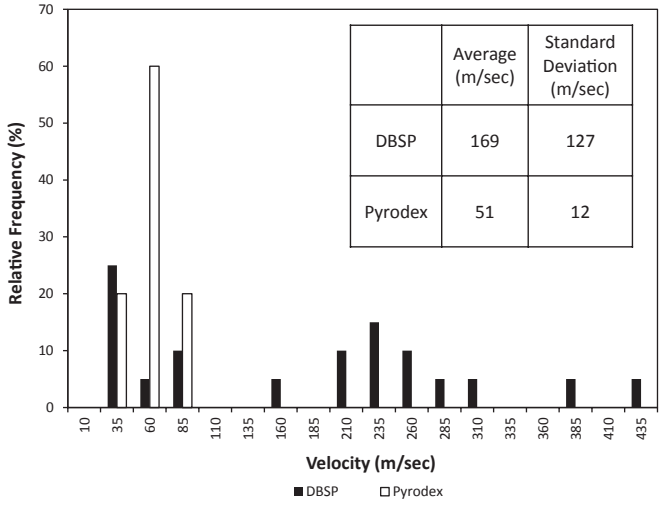

	Average (m/sec)	Standard Deviation (m/sec)
DBSP	169	127
Pyrodex	51	12

FIG. 4—*Histogram of fragment velocities from galvanized steel devices filled with either double-base smokeless powder (DBSP) or Pyrodex.*

Given that high-speed photography was used to capture the explosion event, a stepwise sequence of the bombs exploding was able to be captured. Figures 5 and 6 show the PVC DBSP devices over a time period of 1500 μs. The point of first failure was along the body of the pipe at a time equal to approximately 600 μs for both devices. The paths of specific fragments were then mapped using PVVMs. Figures 7 and 8 show the PVVMs of the two PVC DBSP devices, where the devices exhibit severe fragmentation with a wide range of velocities. Note that a cluster of slower-moving fragments appears at positions and trajectories suggesting they emanated from the right endcap, in which the igniter wires were inserted.

Figure 9 illustrates the photographic sequence of the explosion of black steel with DBSP. The point of first failure can be seen as the endcap opposite the igniter wires, with the entire explosion event occurring within 500 μs. The PVVM for this device, shown in Fig. 10, demonstrates a wide range of fragment velocities and trajectories. As was seen previously, a cluster of slow-moving fragments appears to track back to the right endcap. In addition, one of the fragments in the video sequence had a distinctive shape, so that it could be tracked as well as recovered and weighed. The trajectory for this fragment is labeled in the PVVM (see below for more discussion on this fragment).

Figure 11 displays the galvanized steel DBSP device, which begins to fail at 100 μs, and the explosion is complete within 500 μs. As was seen with the black steel device, the point of first failure was at the endcap (although in this case, it was the end cap with the igniter wires). Figure 12 shows the path of the fragments in all directions from the pipe, as well as velocities falling between 20 and 435 m/sec. The pattern of slow-moving fragments emanating from the drilled end of the device is also evident.

Figure 13 displays the PVC Pyrodex device explosion with the first failure of the pipe body shown in the second frame. Figure 14 shows the PVVM of the same device, with fragments escaping in all directions, including many originating from the right endcap. These fragments were positively identified in the video as multiple fragments of the right end cap. Figure 15 depicts the progression of the black steel Pyrodex explosion. Note the first failure at time 100 μs on the right endcap. It is evident from Figure 16 that a smaller number of fragments were able to be traced, due to the less complete fragmentation caused

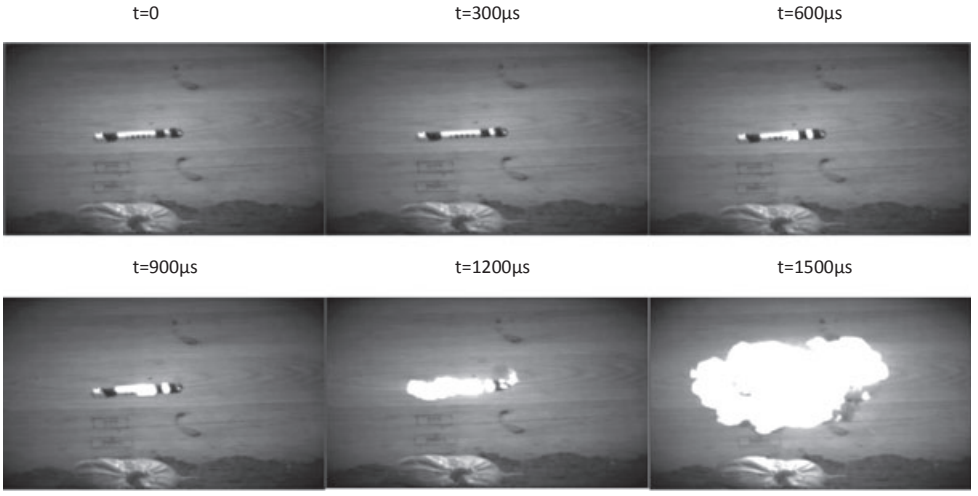

FIG. 5—*Stepwise frames of the first PVC double-base smokeless powder (DBSP) device exploding over 1500 µs.*

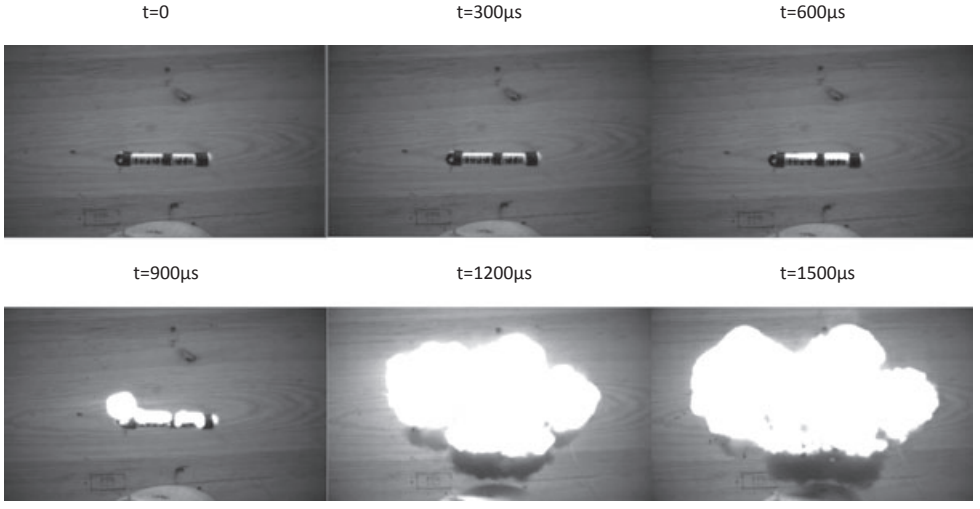

FIG. 6—*Stepwise frames of the second PVC double-base smokeless powder (DBSP) device exploding over 1500 µs.*

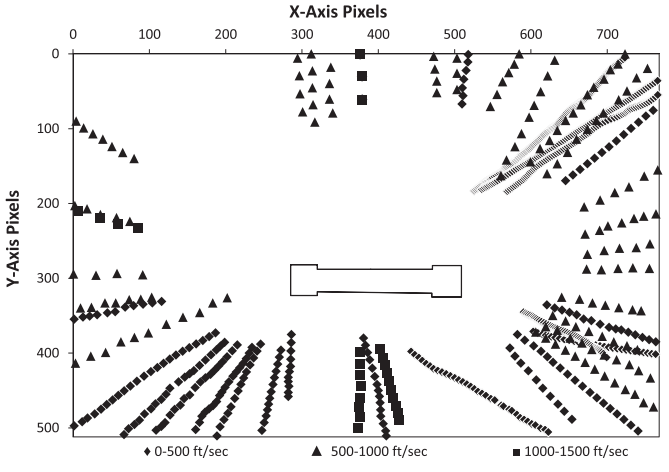

FIG. 7—*Particle velocity vector map (PVVM) of the first PVC pipe filled with double-base smokeless powder (DBSP).*

by the lower energy filler. The pipe body itself was tracked due to its large size and slow velocity. Figure 17 shows the progression of the galvanized steel Pyrodex explosion. Note the first failure at the right endcap, as well as the subsequent failure at the other endcap. Once again, few particles were tracked in the lower energy filler devices. Figure 18 shows a "banana peel" fragment, which is a characteristic fragmentation pattern for low energy explosives such as Pyrodex.

Mass Measurements

Table 1 summarizes the slopes of the FWDM plots of the various devices, along with the corresponding R^2 values. Fitting a FWDM to a line is problematic due to significantly larger fragments, which tend to dictate the slope. Regardless, when including all fragments in the slope determination, the behavior of the energetic fillers agrees with previously published results. For example, DBSP has a much steeper slope demonstrating more fragmentation overall, indicating a higher energy filler. On the other hand, Pyrodex exhibits a shallow slope caused by the presence of large fragments, characteristic of lower energy fillers. For the PVC DBSP slope calculation, two devices were included; however, the results still follow Oxley's model. The metal Pyrodex devices also corresponded with Oxley, despite exceptionally low linearity values of 0.6401 and 0.5162 for

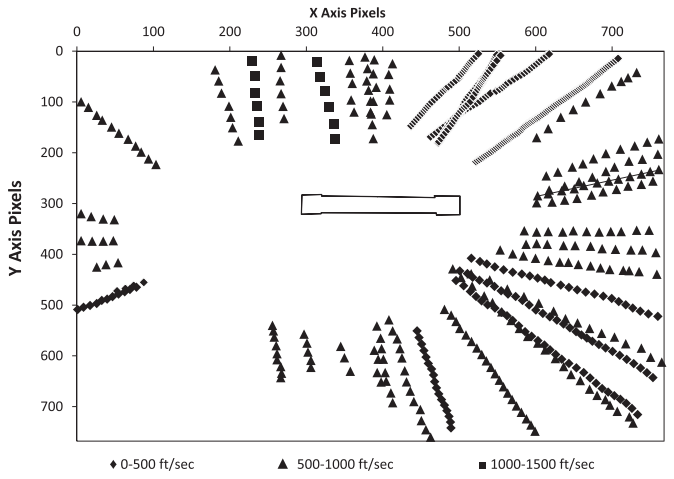

FIG. 8—*Particle velocity vector map (PVVM) of the second PVC pipe filled with double-base smokeless powder (DBSP).*

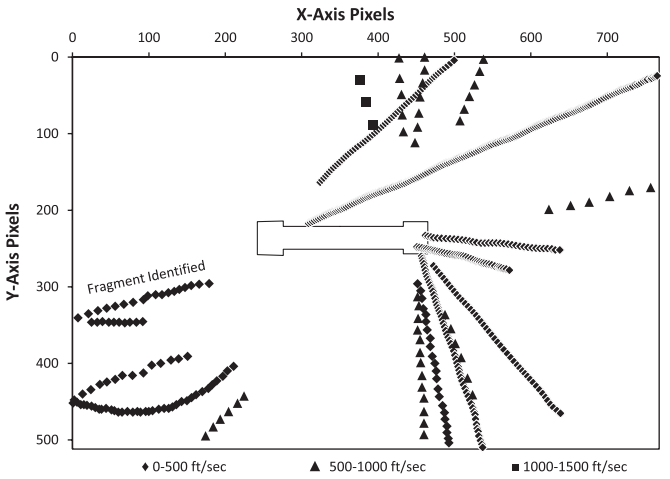

FIG. 10—*Particle velocity vector map (PVVM) of the black steel pipe filled with double-base smokeless powder (DBSP).*

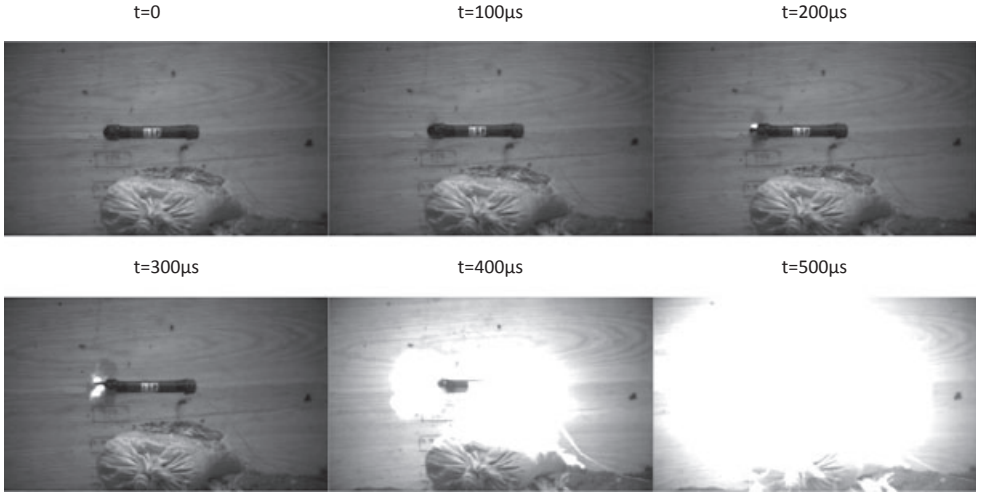

FIG. 9—*Stepwise frames of the black steel double-base smokeless powder (DBSP) device exploding over 500 µs.*

black steel and galvanized steel, respectively. Incomplete fragmentation of these devices produced relatively large fragments; therefore, this produced a wide range of masses and ultimately poor linearity. Removing these points dramatically improved the correlation values to near 0.97. However, by doing so, the black steel devices deviated from Oxley's model, with the Pyrodex device having a steeper slope than the DBSP device.

In addition to the FWDMs, histograms were generated to show fragment mass distribution. The plots reinforce the information gained from the FWDM slope values. The PVC histogram (Fig. 19) shows that the heaviest fragment from the DBSP device is located at 5% by mass, signaling complete fragmentation. The Pyrodex fragments were concentrated near the lowest bin, with decreasing amounts in each of the successive bins with the heaviest fragment being 9% by mass. Once again, the histogram comparing the fillers in a black steel pipe (Fig. 20) supports the information from the FWDM. Both the DBSP and Pyrodex produced a fragment considerably larger than the others, 32% and 65% by mass, respectively. The significant difference in these values is shown by the histogram as well as the photographs. The galvanized steel pipe filled with Pyrodex produced a large fragment that showed peeling, easily seen in the photograph in Fig. 21, which heavily influenced the slope of the FWDM. In comparison, the masses of the DBSP pipe were all relatively similar, with the heaviest fragment being 20% by mass.

Momentum and Kinetic Energy Calculations

One important observation brings together several aspects of this study. Fortunately, the DBSP black steel device contained a fragment whose unique shape allowed for it to be easily recognized in the video. The same fragment was then recovered from one of the walls of the enclosure and weighed. As a result, both the velocity and mass of the fragment were known (104.9 m/sec and 48.76 g, respectively). Therefore, the momentum and kinetic energy of the fragment could be calculated. For example, the momentum of this fragment was 5.11 kg-m/sec, and its kinetic energy was 268 J. By way of comparison, a 0.45 caliber bullet weighs much less but travels faster. As a result, such a bullet yields less momentum (3.79 kg-m/sec) but more kinetic energy (483 J). Finally, this particular fragment was also spinning as it flew away from the site of the explosion at *c.* 25,000 revolutions per minute (rpm), which vastly exceeds the rpm of an automobile engine and is more comparable with tools like metal grinders. Locating this fragment was quite fortuitous–we were not

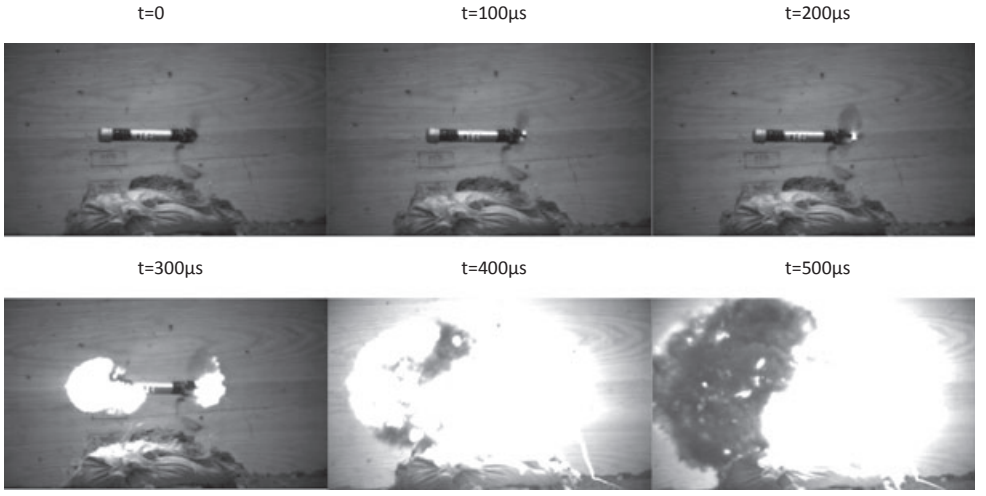

FIG. 11—*Stepwise frames of the galvanized steel double-base smokeless powder (DBSP) device exploding 500 µs.*

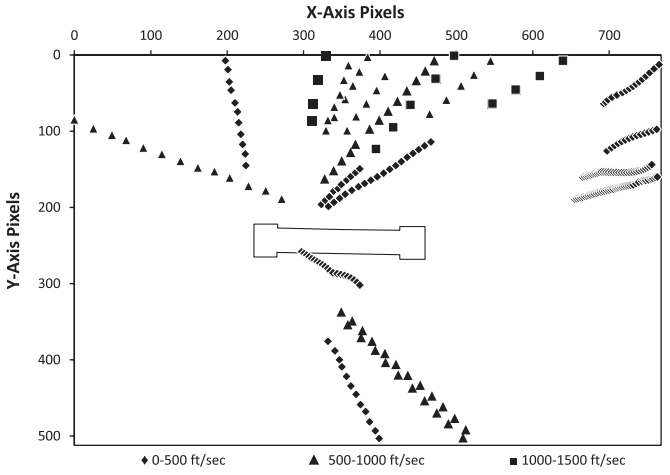

FIG. 12—*Particle velocity vector map (PVVM) of the galvanized steel pipe filled with double-base smokeless powder (DBSP).*

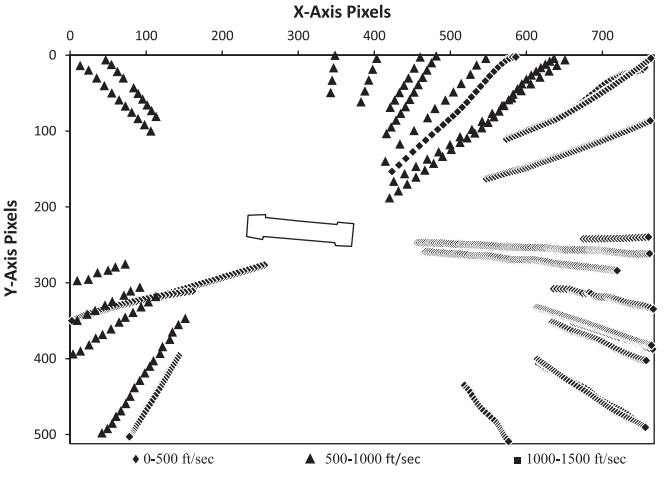

FIG. 14—*Particle velocity vector map (PVVM) of the PVC pipe filled with Pyrodex.*

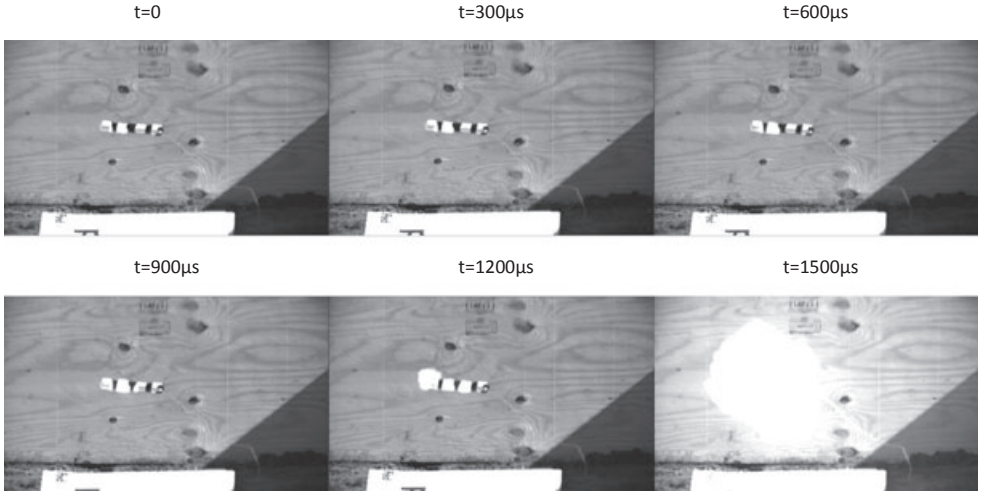

FIG. 13—*Stepwise frames of the PVC Pyrodex device exploding over 1500 µs.*

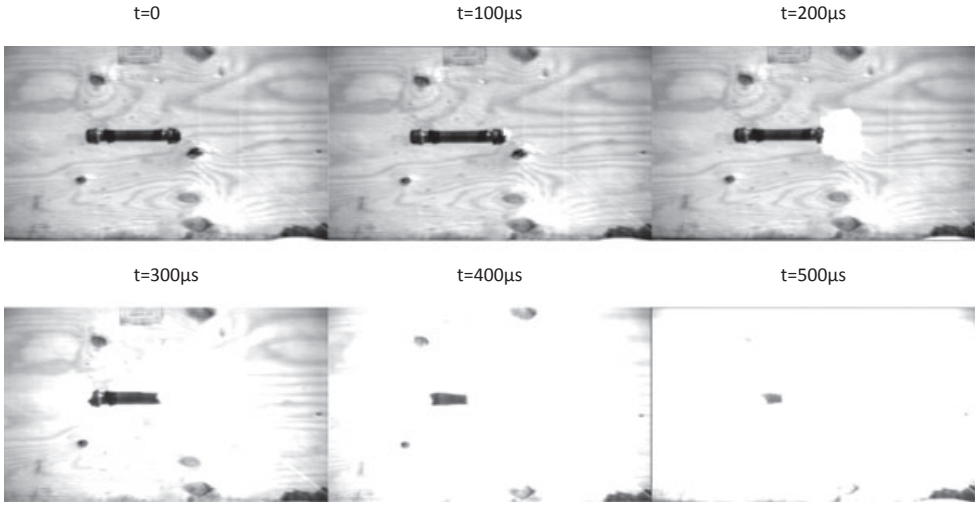

FIG. 15—*Stepwise frames of the black steel Pyrodex device exploding over 1500 µs.*

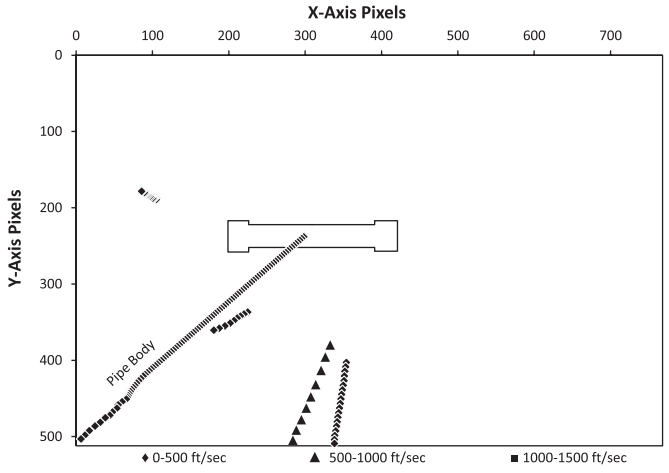

FIG. 16—*Particle velocity vector map (PVVM) of the black steel pipe filled with Pyrodex.*

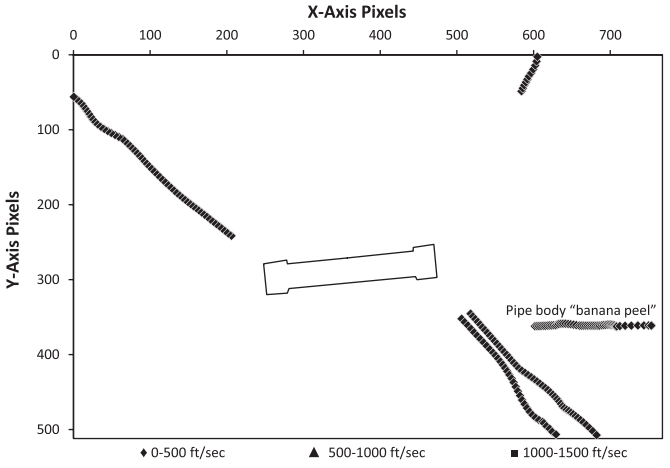

FIG. 18—*Particle velocity vector map (PVVM) of the galvanized steel pipe filled with Pyrodex.*

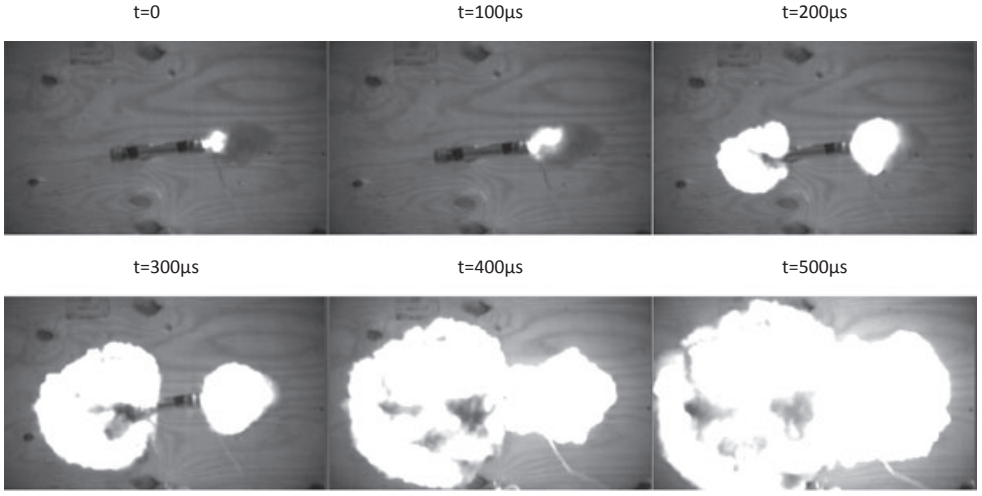

FIG. 17—*Stepwise frames of the galvanized steel Pyrodex device exploding over 500 µs.*

TABLE 1—*Comparison of slopes of FWDMs for all devices.*

Type of Pipe	Type of Filler	Slope of FWDM (Including All Points)	R^2	*n*
PVC (2 devices)	DBSP	−47.4 ± 0.9	0.8642	393
Black Steel	DBSP	−1.48 ± 0.07	0.9587	24
Galvanized Steel	DBSP	−2.5 ± 0.2	0.8826	18
PVC	Pyrodex	−14.1 ± 0.3	0.9426	190
Black Steel	Pyrodex	−0.27 ± 0.06	0.6401	11
Galvanized Steel	Pyrodex	−0.14 ± 0.05	0.5162	11

FWDMs, Fragment Weight Distribution Maps; PVC, polyvinyl chloride.

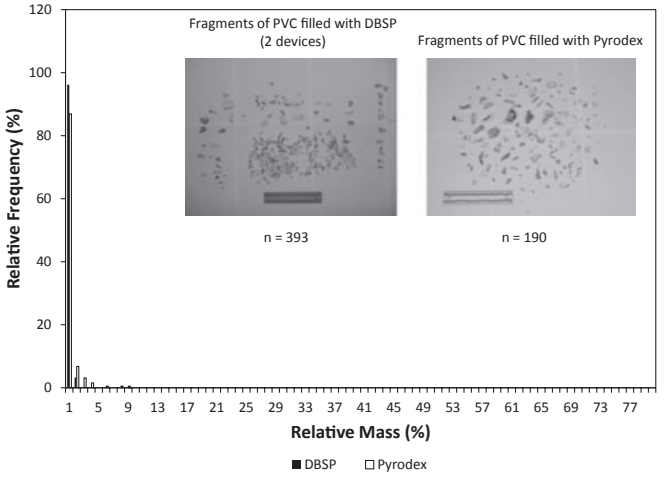

FIG. 19—*Histogram of fragment masses from PVC devices filled with either double-base smokeless powder (DBSP) or Pyrodex.*

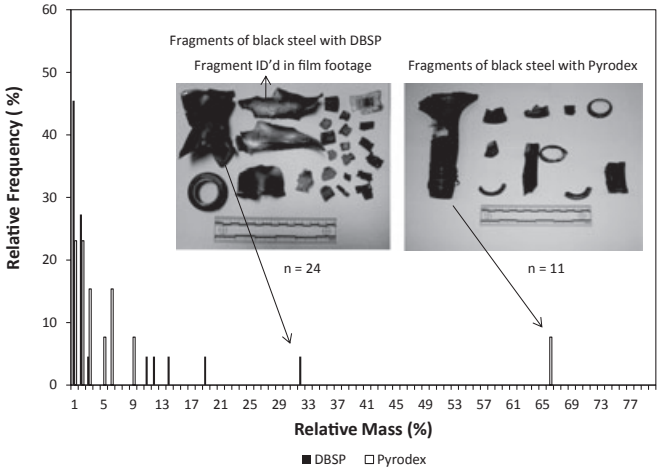

FIG. 20—*Histogram of fragment masses from black steel devices filled with either double-base smokeless powder (DBSP) or Pyrodex.*

able to identify any other fragments for which velocity and mass were known.

Conclusions

Based upon high-speed videography, and with all pipe types, the highest overall velocities were observed with the DBSP filler. In fact, the velocities of the fastest fragments in this study are comparable with the muzzle velocities of handgun projectiles. In addition, all devices except the metal devices containing Pyrodex had clusters of low-velocity fragments near the right endcap. This could be characteristic of endcap material that did not experience the same internal pressure. This would occur if a small but significant amount of gas was allowed to escape through the drill hole. For metal devices, the first failure occurred at the endcaps, but for the PVC devices, the pipe body was the point of failure. Additionally, the PVC devices took nearly three times as long to explode compared with the metal devices. In general, the Pyrodex devices exhibited lower overall velocities clustered in a narrow range. This is in stark contrast to DBSP, which produced higher-velocity fragments over a broad range. The mass of the fragments was a clear indication of filler both in terms of the FWDM but also some general trends in metal pipes, where the Pyrodex devices were the only ones that contained a fragment that represented more than 50% of the total mass recovered.

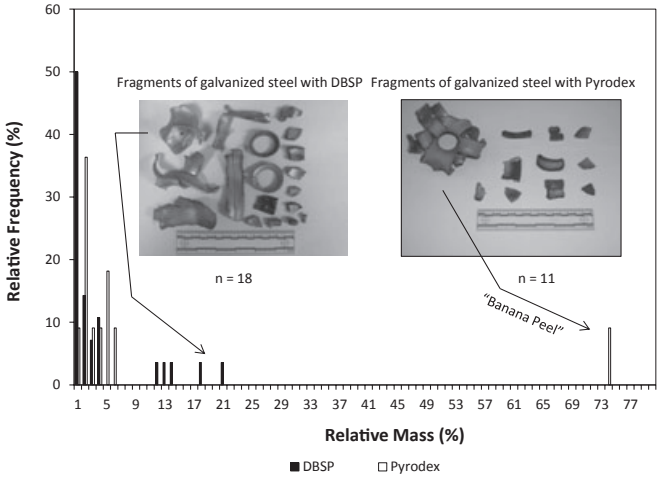

FIG. 21—*Histogram of fragment masses from galvanized steel devices filled with either double-base smokeless powder (DBSP) or Pyrodex.*

Acknowledgments

The authors would like to thank Sergeant Leonard Langland and the members of the Indiana State Police Bomb Squad, as well as Special Agent Donald Sachtleben of the Federal Bureau of Investigation for ensuring the safety of all participants, as well as assembling and initiating all explosive devices. The authors also acknowledge Bever Gravel, Inc. for providing a location for the blasts to occur. Steve Stahlhut, Ron Jones, and John Huhn of Motion Engineering Corporation were extremely helpful in terms of consulting, training, and utilization of the high-speed video equipment. Finally, the authors acknowledge all undergraduate and graduate students at IUPUI who assisted at the explosion event.

References

1. Lucas J, Crane J. Fatalities associated with home-made pipe bombs in Northern Ireland. Am J Forensic Med Pathol 2008;29(2):93–8.
2. Lardner G, Adams L. To unabomb victims, a deeper mystery. Washington Post 1996 April 14; page A01; http://www.washingtonpost.com/wp-srv/national/longterm/unabomber/bkgrdstories.victims.htm.
3. ATF. Expertise on improvised explosives devices (IEDs), 2013; http://www.atf.gov/publications/factsheets/factsheet-IED.html.
4. Beveridge A, editor. Forensic investigation of explosives. Bristol, PA: Taylor and Francis, 1998.

5. Midkiff CR. Arson and explosives investigation. In: Saferstein R, editor. Forensic science handbook, 2nd edn. Upper Saddle River, NJ: Prentice Hall, 2002.
6. Yinon J. Analysis of explosives by LC/MS. In: Yinon J, editor. Advances in forensic applications of mass spectrometry. New York, NY: CRC Press, 2004;243–86.
7. Marshall M, Oxley JC, editors. Aspects of explosives detection. New York, NY: Elsevier, 2009.
8. Taylor GI. The fragmentation of tubular bombs. Scientific Papers 1944; 3(44):387–90.
9. Al-Hassani STS, Hopkins HG, Johnson W. A note on the fragmentation of tubular bombs. Int J Mech Sci 1969;11(6):545–9.
10. Hoggatt CR, Recht RF. Fracture behavior of tubular bombs. J Appl Phys 1968;39(3):1856–62.
11. Anderson CE, Predebon WW, Karpp RR. Computational modeling of explosive-filled cylinders. Int J Engng Sci 1985;23(12):1317–30.
12. Taylor GI. Analysis of the explosion of a long cylindrical bomb detonated at one end. Scientific Papers 1941;2:277–86.
13. Formulae for Ammunition Management. UNODA; 2011 Oct. Report No.: IATG 01.80:2011[E].
14. Oxley JC, Smith JL, Resende E, Rogers E, Strobel RA, Bender EC. Improvised explosive devices: pipe bombs. J Forensic Sci 2001;46 (3):510–34.
15. Dean R, Edwards MR. Fragment distribution as an aid to forensic failure investigations at the scene of explosions. J Fail Anal and Preven 2002;2 (2):33–40.
16. Held M, Kuhl P. Consideration to the mass distribution of fragments by natural-fragmentation in combination with preformed fragments. Propell Explos Pyrot 1976;1:20–3.
17. Walsh GA, Inal OT, Romero VD. A potential metallographic technique for the investigation of pipe bombings. J Forensic Sci 2003;48(5): 945–60.
18. Gregory O, Oxley JC, Smith J, Platek M, Ghonem H, Bernier E, et al. Microstructural characterization of pipe bomb fragments. Mater Charact 2010;61(3):347–54.

Additional information and reprint requests:
John V. Goodpaster, Ph.D.
Forensic and Investigative Sciences Program
Department of Chemistry and Chemical Biology
IUPUI
402 North Blackford Street
Indianapolis, IN 46202
E-mail: jvgoodpa@iupui.edu